J. Fluid Mech. (1996), vol. 328, pp. 253–269

Diffusion in stably stratified turbulence

By Y. KIMURA[1,2]† AND J. R. HERRING[1]

[1]National Center for Atmospheric Research, PO Box 3000, Boulder, CO 80307, USA

[2]Program in Applied Mathematics, University of Colorado, Campus Box 526, Boulder, CO 80309-0526, USA

(Received 29 September 1995 and in revised form 19 June 1996)

We examine results of direct numerical simulations (DNS) of homogeneous turbulence in the presence of stable stratification. We focus on the effects of stratification on eddy diffusion, and the distribution of pairs of particles released in the flow. DNS results are presented over a range of stratification, and at Reynolds numbers compatible with aliased free spectral results for a resolution of 128^3 mesh points. We compare results for particle dispersion to simple analytic theories such as that proposed by Csanady (1964) and Pearson *et al.* (1983) by adapting the basic Langevin model to decaying turbulence at low Reynolds numbers. Stable stratification is found to arrest both single particle displacements and pair separation in the direction of stratification, but it leaves these quantities nearly unaltered in the transverse direction. With respect to the dynamics of stratified flows, we find that regions of strong viscous dissipation are intermittently spaced, and are associated with large horizontal vorticity, consistent with recent experimental results by Fincham *et al.* (1994).

1. Introduction

In atmospheres and oceans, flows are usually stably stratified. Numerical simulations of such flows play a vital role in improving our understanding of geophysical and astrophysical turbulent phenomena. In particular, diffusion problems in stratified turbulence are not only of scientific and mathematical interest, but are also of practical importance in environmental and industrial research. For example, parameterization of eddy diffusivity with stratification and sometimes rotation is crucial in various atmospheric and ocean models.

The central nature of stratified turbulence is the coexistence of waves and turbulence, between which the kinetic energy is partitioned (Riley, Metcalfe & Weissman 1982; Métais & Herring 1989; Herring & Métais 1989). The latter enhances diffusion by way of eddy transport, while the former contributes to an oscillatory motion of the scalar, with, perhaps, little dispersion. Overall, it is thought that stratification suppresses diffusion in the direction of stratification (for experimental confirmation of this point, see Britter *et al.* 1993, in particular, figure 3).

This paper studies these aspects of diffusion in stably stratified turbulence using direct numerical simulations (DNS). We also examine the dynamics of such flows, their structural features, and single and particle-pair dispersion, utilizing a high-order particle-tracking scheme (Yeung & Pope 1989). The methodology here is the same as

† Present address: Graduate School of Polymathematics, Nagoya University, Nagoya 464-01, Japan.

in a previous report (Kimura & Herring 1995) which discussed results of calculations with 64^3 grid points. This paper extends the discussion to a resolution of 128^3.

The suppression of diffusion in the direction of stratification was theoretically predicted by Csanady (1964) with an heuristic stochastic modelling of the pressure term in the Navier–Stokes equation. For stationary turbulence, he proposed a Langevin model with an exponential form for the velocity auto-correlation function, and a linear incorporation of buoyancy effects in the stratified direction. Comparison of his theory with decaying turbulence simulations is another purpose of this paper.

We analyse numerical results with simple scaling laws and underlying concepts drawn from the statistical theory of turbulence. Such statistical ideas are cleanest at asymptotically large Reynolds numbers, a domain remote from DNS. However, the basic assumptions of the statistical theory apply equally, and perhaps better, to low-Reynolds-number, rapidly decaying flows, and in this paper we check to see to what degree DNS and statistical theory agree at low Reynolds numbers ($R_\lambda \sim 20$). Our method is to use the statistical theory to extract the functional dependence of dispersive effects on turbulence spectra and other parameters, and to compare these to the DNS results. Numerical results are provided in §3, and analysis is given in §4, after a description of simple statistical predictions for eddy diffusion and particle dispersion in the presence of stable stratification. Section 5 presents a summary of our results, and §6 states our conclusions.

2. Methodology

The (non-dimensionalized) Navier–Stokes equations within the Boussinesq approximation,

$$(\partial_t - \nu\nabla^2)\boldsymbol{u} = -\boldsymbol{u}\cdot\nabla\boldsymbol{u} - \nabla p + \theta\hat{z}, \tag{2.1}$$

$$(\partial_t - \kappa\nabla^2)\theta = -N^2 w - \boldsymbol{u}\cdot\nabla\theta, \tag{2.2}$$

$$\nabla\cdot\boldsymbol{u} = 0, \tag{2.3}$$

are solved in a 2π-periodic box (128^3 grid points) using the pseudo-spectral method with the 2/3 rule for de-aliasing. (We recall that such methods are equivalently Galerkin, since the 2/3 rule eliminates aliasing errors (Orszag & Patterson 1972).) Our notation is that $\boldsymbol{u}$ is the velocity, whose (x, y, z) components are (u, v, w), and θ is the temperature fluctuation about the linear (stable) mean temperature profile $\mathrm{d}\overline{T}/\mathrm{d}z \equiv -N^2$). N is the Brunt–Väisälä frequency, $(g\alpha(\partial\overline{T}/\partial z)/T_0)^{1/2}$. Here, $\alpha = \{\mathrm{d}\ln(\rho)/\mathrm{d}\ln(T)\}_P$. Periodic boundary conditions are used in the calculation for $\boldsymbol{u}$ and θ by assuming a linear ambient density profile. For the time advancement, the low-storage third-order Runge–Kutta method by A. A. Wray is used.

Particle trajectories are computed by solving $\mathrm{d}\boldsymbol{X}_j(t)/\mathrm{d}t = \boldsymbol{u}(X_j, t)$ using the same time-marching scheme as with the velocity. Cubic spline interpolation is used to get the necessary fine-scale information for $\boldsymbol{X}_j(t)$ (Yeung & Pope 1989). Because of periodic boundary conditions, we can use the fast Fourier transform for solving the tridiagonal matrix equation for the spline function. The DNS consists of an initial Gaussian random isotropic velocity field which has a three-dimensional energy spectrum given by

$$E(k) = 16(2/\pi)^{1/2}u_0^2 k_0^{-5}k^4\exp(-2(k/k_0)^2) \tag{2.4}$$

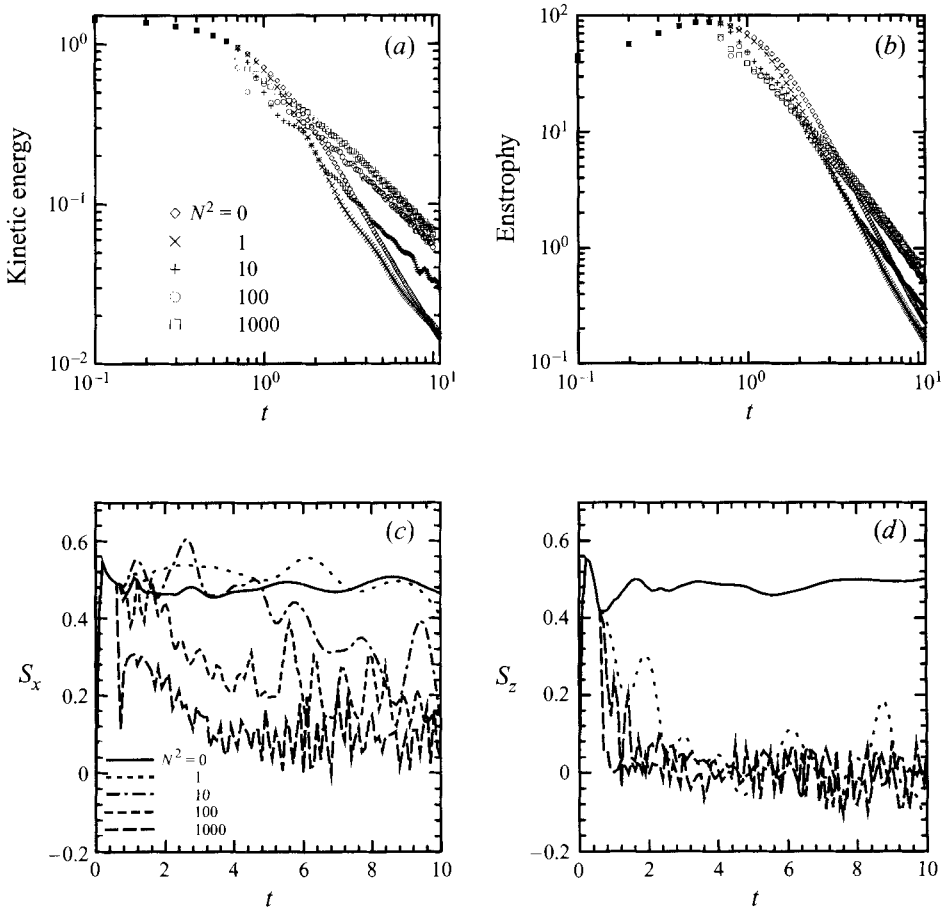

FIGURE 1. Statistics of the velocity field for $N^2 = 0$, 1, 10, 100, 1000. (*a*) The kinetic energy, (*b*) the enstrophy, (*c*) the skewness of $\partial u/\partial x$, (*d*) the skewness of $\partial w/\partial z$.

with $k_0 = 4.767$ and $u_0 = 1.242$. (The basic code and numerical procedure is described in Kimura 1992.) The kinematic viscosity $\nu = 0.005$, and the Prandtl number $P_r \equiv \nu\,\kappa = 1$. The initial Taylor-microscale Reynolds number is ~ 84. Starting with decaying turbulence, stratification and temperature fluctuations are introduced after the enstrophy reaches its peak value at $t \sim 0.6$. By this time, the velocity derivative skewness has reached its maximum value of ~ 0.5 (figure 1). Both facts imply that small scales are fully developed by the time stratification is introduced (at $t = 1.0$). In addition, by this time, small-scale truncation errors (aliasing) have had a chance to dissipate.

Lagrangian particles are released at $t = 1$. A total of $13824 = 24^3$ pairs of particles are used to get clean Lagrangian statistics. Initially, one set of particles is located at regularly spaced three-dimensional grid points, $\boldsymbol{x}_j(0)$ and the other set of particles is placed at $\boldsymbol{x}_j + \Delta\boldsymbol{x}_j$, where $\Delta\boldsymbol{x}_j = (d, 0, 0)$ and $d = 0.005$. If measured by the dissipation scale $\eta_0 = (\nu^3/\epsilon)^{1/4}$ at $t = 0.6$, this initial displacement d corresponds to $0.257\eta_0$. The small values of skewnesses found here are consistent with the tendency for velocity gradients to become Gaussian with increasing N, as reported by Métais & Herring (1989).

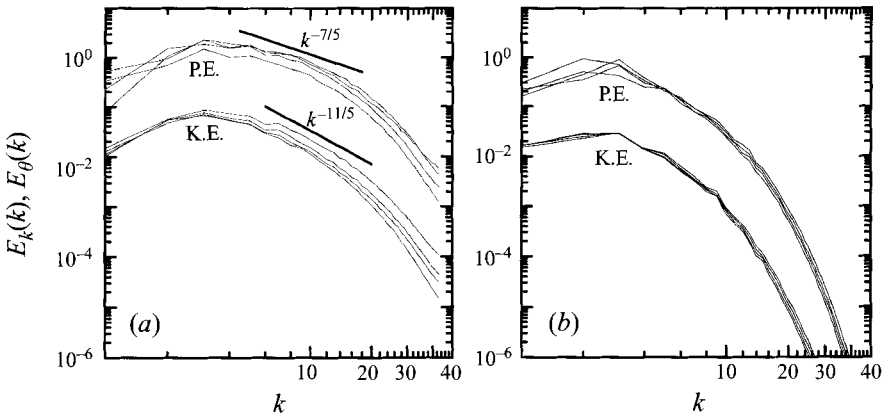

FIGURE 2. The kinetic and potential energy spectra for $N^2 = 100$. (Potential energy is not normalized by N^2.) (*a*) t is from 1.0 to 1.6, and (*b*) t is from 5.0 to 5.6. The time interval of plots is 0.2.

3. Numerical results

Figure 1 summarizes the overall statistics of turbulence for $N^2 = 0$, 1, 10, 100, and 1000. (Hereafter, the label $N^2 = 0$ means the turbulence is uncoupled from both the mean and fluctuation temperature fields.) Both kinetic energy,

$$E_{kin} = \sum_{k} \frac{1}{2} \mid \boldsymbol{u}(\boldsymbol{k}) \mid^2 \tag{3.1}$$

and enstrophy

$$D = \sum_{k} k^2 \mid \boldsymbol{u}(\boldsymbol{k}) \mid^2 \tag{3.2}$$

decay almost as a power of time ($E(t) \sim t^{-p}$), with some oscillatory fluctuations due to conservative energy exchange between kinetic and potential energy. We denote the latter by

$$E_{pot} = \sum_{k} \tfrac{1}{2} \mid \theta(\boldsymbol{k}) \mid^2 / N^2. \tag{3.3}$$

The value of p becomes smaller with increasing N. This fact is consistent with the faster decay of the skewness factor of the longitudinal velocity gradient field $\partial u/\partial x$:

$$S_x = -\langle(\partial u/\partial x)^3\rangle / \langle(\partial u/\partial x)^2\rangle^{3/2}, \tag{3.4}$$

which is a measure of the energy cascade to smaller scales. S_x is shown in figure 1(*c*). The decay of S in the vertical direction is significant if there is stratification, and thus the inhibition of the energy cascade to smaller scales keeps the kinetic energy from the dissipation range. This observation goes back to Riley *et al.* (1982).

The inhibition of the energy cascade is also reflected in the fact that the energy spectrum becomes steeper with increasing N. Typical spectra for $E_{kin}(k)$ and $E_{pot}(k)$ are shown in figure 2. These spectra have been spherically averaged over wavenumber bins of unit radial thickness. Two time slots are shown for $N^2 = 100$: one around $t = 1.0$, when S_z is sharply dropping (figure 2*a*), and the other around $t = 5.0$, by which time S_z has fallen and begun oscillating around zero (figure 2*b*). (The potential energy (shown in figure 2*b*) is not divided by $N^2 = (100)$). In figure 2(*a*), lines are shown which correspond to the Bolgiano–Obukhov spectra of kinetic energy and

temperature fluctuation predicted for stratified turbulence ($E_{kin}(k) \sim k^{-11/5}$, $E_{pot}(k) \sim k^{-8/5}$). Although spectra with similar slopes can be observed for a small range of wavenumbers at earlier times, soon they are overtaken by the dissipation spectra (a near-exponential range), and thus it is not conclusive whether the Bolgiano–Obukhov physics operates for the present low-Reynolds-number decaying flow. At high wavenumbers, the kinetic and potential energies show the same slope, and if the latter is normalized by $N^2 = 100$, they are equipartitioned. (Strong anisotropy may exist in the large-scale velocity field, and then presenting horizontal and vertical spectra separately may be more appropriate (Métais & Herring 1989).)

As noted above, both the steepness of the kinetic energy spectrum and the smaller value for p for the decay of the total energy may be related to the cascade reduction induced by stratification. Simple closure estimates of the EDQNM sort also suggest this. The essence of such a theory is that energy transfers to progressively smaller scales (of size $2\pi/k$) because of their straining by somewhat larger scales. Such strain is imagined to be a stochastic process, and we shall call the duration of straining events $\eta^{-1}(k)$. For isotropic turbulence, $\eta(k) \sim (\int_0^k p^2 \mathrm{d}pE(p))^{1/2}$, while for strongly stratified turbulence, an effective value of $\eta(k) \sim N$ is plausible. (A more quantitative discussion of these issues is to be found in Godeferd & Cambon 1994.)† At any rate, if the cascade of energy to small scales is local (as supposed, for example, by Leith 1967), the time development of the energy spectrum, $E(k)$ is determined by

$$(\partial_t + 2\nu k^2)E = \partial_k\{k^4\partial_k\{E(k)\eta(k)/k^2\}\}. \tag{3.5}$$

From (3.5) follows $E(k) \sim \epsilon^{2/3}k^{-5/3}$ for $\eta(k) \sim (\int_0^k \mathrm{d}pp^2E(p))^{1/2}$, and

$$E(k) \sim (\epsilon N)^{1/2}/k^2 \tag{3.6}$$

for strong stratification (Herring 1988). Scaling laws such as (3.6) have been proposed (Zhou 1995) and confirmed (Yeung & Zhou 1995) for rotation turbulence. In that case, the rotation rate replaces N in (3.6). We expect that (3.6) would describe a largely two-dimensional spectrum that would blend into an isotropic $k^{-5/3}$ range as k increases beyond $k_O = ((N^3/\epsilon))^{1/2}$.

We may also estimate the effects for the derivative skewness of the velocity field from (3.5). For isotropic turbulence, $S \equiv \int \mathrm{d}kk^2T(k) \sim 1$, and again ignoring possible effects of anisotropy‡, we find that for strongly stratified turbulence

$$S \sim \left(\int_0^\infty \mathrm{d}kk^2E(k)\right)^{1/2} \Big/ N \tag{3.7}$$

Thus, the DNS results seem to be roughly in qualitative agreement with such simple theoretical estimates.

If we now assume that spectrum (3.6) extends to a wavenumber k_1, below which

† To see how the Brunt–Väisälä frequency enters the statistical formalism, we rewrite (2.1)-(2.3) in a more symmetric form by rescaling the temperature field $\psi \to \theta/N$, and then introducing the Craya representation of $\boldsymbol{u}(\boldsymbol{k}) = \boldsymbol{e}_1(\boldsymbol{k})\phi_1(\boldsymbol{k}) + \boldsymbol{e}_2(\boldsymbol{k})\phi_2(\boldsymbol{k}), \boldsymbol{e}_1(\boldsymbol{k}) = \boldsymbol{k} \times \hat{\boldsymbol{g}}/ \mid \boldsymbol{k} \times \hat{\boldsymbol{g}} \mid$, $\boldsymbol{e}_2(\boldsymbol{k}) = \boldsymbol{k} \times (\boldsymbol{k} \times \hat{\boldsymbol{g}})/ \mid \boldsymbol{k} \times (\boldsymbol{k} \times \hat{\boldsymbol{g}}) \mid$. The variable $\mathscr{Z} \equiv \phi_2(\boldsymbol{k}) + \sqrt{-1}\psi(\boldsymbol{k})$ satisfies an equation of the form $\dot{\mathscr{Z}} = \sqrt{-1}\,\Omega\mathscr{Z} + \mathscr{F}(\mathscr{Z}, \phi_1, \phi_2)$, where $\mathscr{F}$ is that bilinear functional of its arguments that stems from advection and pressure effects. Here $\Omega = N\sin(\vartheta)$. If the EDQNM model of turbulence is implemented on this equation, the eddy-damping rate is changed from its isotropic form $\eta(k)$ to $\eta(k) + (-1.4\Omega)^{1/2}$. Because the gravity waves are dispersive (frequency $\sim N\sin(\vartheta)$, their effect on energy transfer is $\sim (\eta^2 + N^2)^{1/2}$.

‡ Although it may be argued that anisotropy for the small scales which contribute to S_2 is not vital, since turbulence becomes progressively more isotropic with increasing k.

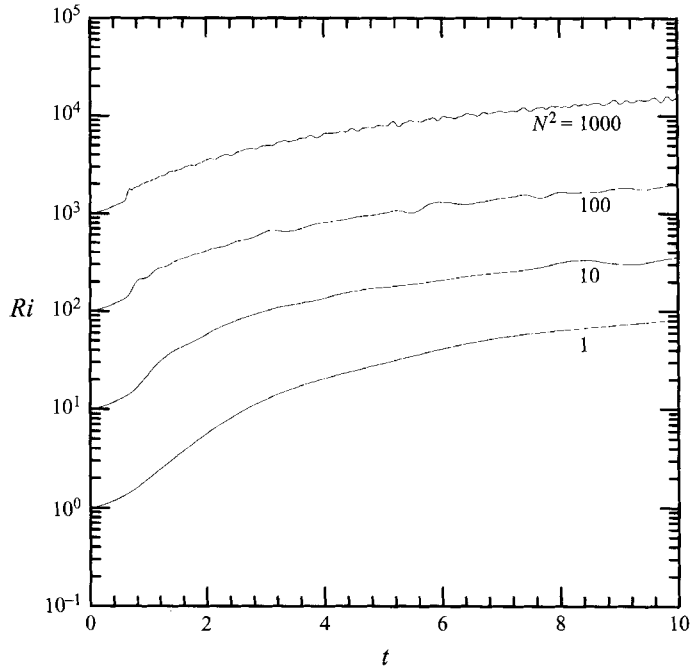

FIGURE 3. The Richardson number as a function of time for N^2 =1, 10, 100, 1000.

the initial spectral shape $E(k) \sim k^4$ persists, and join its shape continuously with (3.6), we may deduce the decay of total energy by using $\dot{E}(t) = -\epsilon$ to find

$$E(t) \sim t^{-5/7}. \tag{3.8}$$

Note that the same analysis applied to isotropic turbulence leads to the law $E(t) \sim t^{-10/7}$, as originally proposed by Kolmogorov (1942), and subsequently derived (with the modification $E(t) \sim t^{-1.37}$) by Lesieur & Schertzer (1978) on the basis of the EDQNM. The DNS results indicate that $E(t) \sim t^{-1}$ as $N \to \infty$. It is unclear whether this discrepancy with closure estimates is a low-R_λ result (as for the case in which $N = 0$), or whether the closure is missing an important dynamical component†. We have not considered here the possibility of a saturation spectrum $E_{kin} \sim N^2/k^3$, as would be obtained if wave breaking alone determined the spectrum. Note that this spectrum cannot decay, contrary to DNS. But we cannot argue against the existence of a saturation spectrum at large R_λ, or at least a spectrum with a saturated segment.

Figure 3 shows the time dependence of the Richardson number $Ri = N^2/\langle(\partial u/\partial z)^2\rangle$ for $N^2 = 1$, 10, 100 and 1000. This figure demonstrates that flows are quite stable all the time for all the values of N.

Figure 4 shows the mean square of the vertical displacement, $\langle Z^2\rangle(t)$, of particles from their initial position for N^2 = (0, 1, 10, 100, and 1000). For stationary turbulence, the slopes of such curves would give the eddy diffusion coefficient. We note a pronounced decrease in particle displacement with increasing N. At higher values of N, the curves level off at $\langle Z^2\rangle(t) \sim N^{-2}$. The case is put more dramatically in figure 5, which shows the distribution function for the vertical displacement $z(t)-z(0)$.

† The analysis leading to (3.8) must be modified if $k_1(t)$ encounters the cut-off wavenumber, $k_c = 1$. In that cases, k_1 is fixed, and a reworking of the Lesieur–Schertzer analysis with this constraint does indeed yield $E_{kin}(t) \sim t^{-1}$.

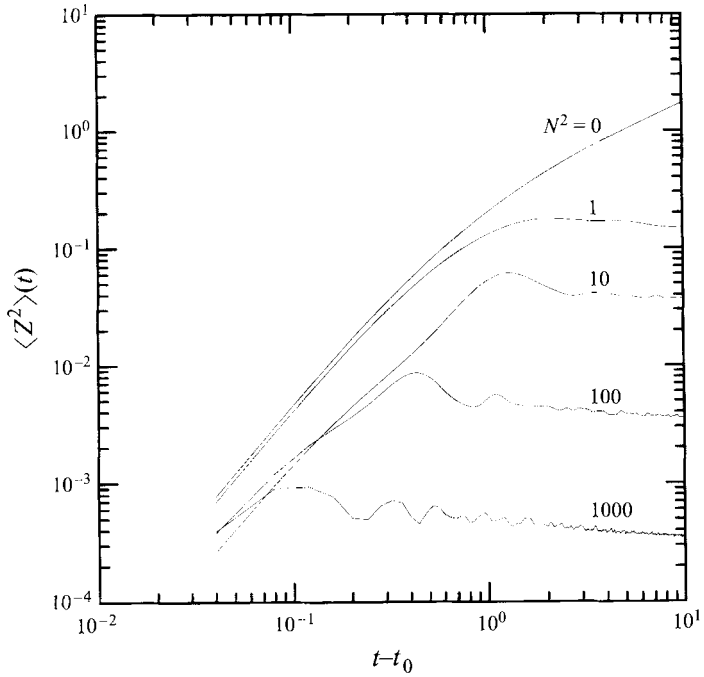

FIGURE 4. The mean square of the vertical displacement $\langle Z^2\rangle(t)$ for $N^2 = 0$, 1, 10, 100, 1000.

Notice that even for modest stratification ($N = 1$), particles cease to migrate in the vertical, and in fact their distributions become slightly more narrow at late times. Similar curves for $\langle X^2\rangle(t)$ and $\langle Y^2\rangle(t)$ show few effects of stratification, and their distribution functions are quite similar to those for unstratified turbulence. Figure 6 shows the r.m.s. of vertical separation of particle pairs,

$$\langle \rho_z^2 \rangle \equiv \frac{1}{n} \sum_{j=1}^{n} (\Delta z_j)^2 \tag{3.9}$$

for $N^2 = 0$, 1, 10, 100, and 1000. Also shown on the figure are straight lines showing the initial Taylor range, $\sim t^1$, the long-time diffusion law, $t^{1/2}$, and the Batchelor range, $t^{3/2}$ in between. At later times, when two particles are almost independent of each other, the curves level off at progressively lower values with increasing N^2. (For $N^2 = 100$ and 1000, the growth is so slow that their values of $\langle Z^2\rangle$ have not reached equilibrium by $t = 10$.) Higher-frequency oscillations are also evident for large stratifications. Of course, we must recall that the value of R_λ for the DNS is too low for inertial effects (which are needed to derive the $t^{3/2}$ regime) to be fully expressed. Hence, the tangential 'agreement' in the Batchelor range is more a matter of a necessary transition between t^1 at short times, and $t^{1/2}$ at long times, than a confirmation of the influence of inertial effects. We should also note that the present study is at low R_λ, whereas the classic time power laws assume that $R_\lambda \to \infty$. Hence, $Z^2(t) \to t$ is not expected.

The dispersion of particles can be related to the Lagrangian auto-correlation function,

$$R_{zz}(\tau, t_0) = \langle w(t_0)w(t_0 + \tau)\rangle / \langle w^2(t_0)\rangle. \tag{3.10}$$

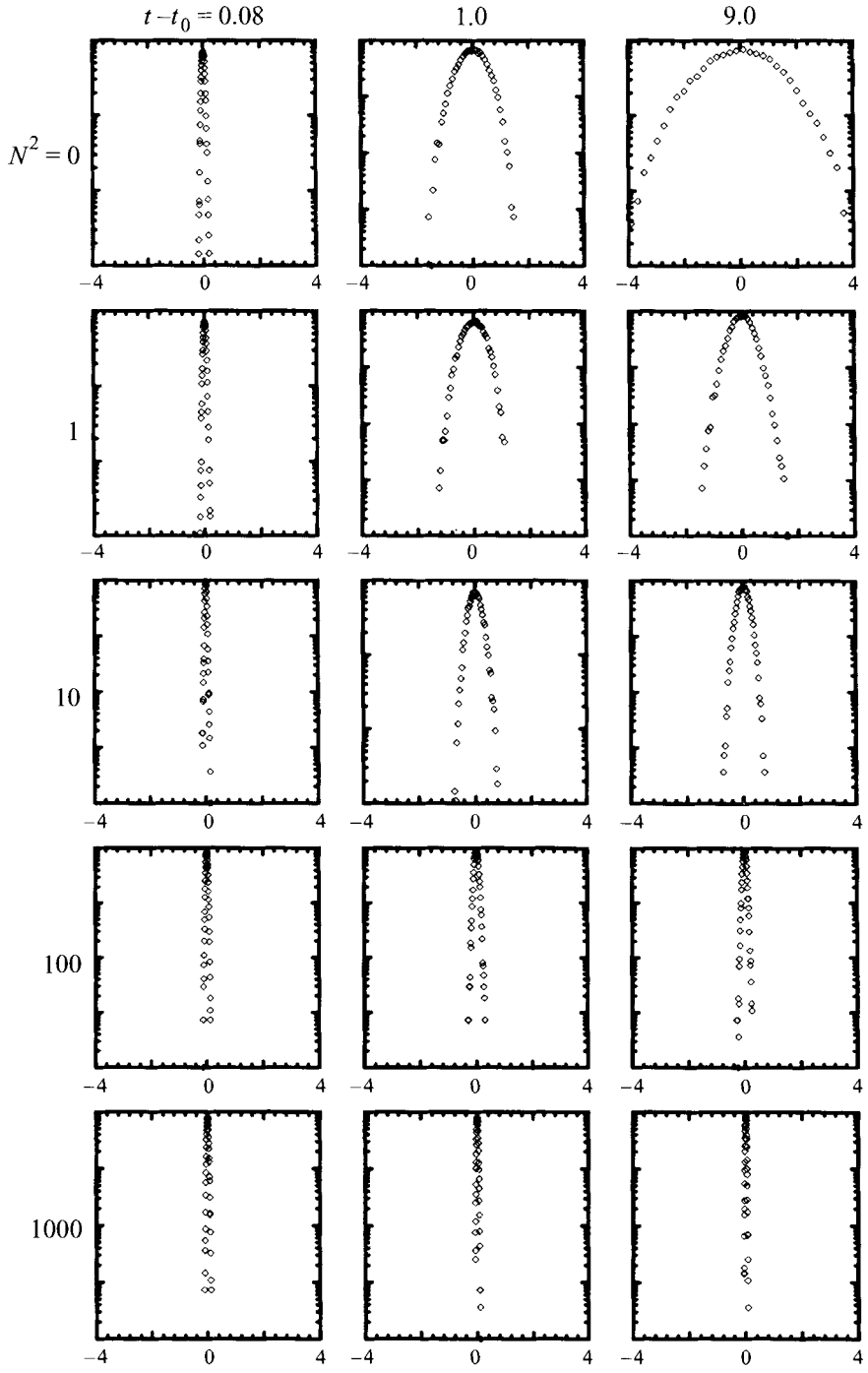

FIGURE 5. Probability distribution of the vertical displacement $z(t) - z(0)$ (unnormalized). The cases for $N^2 = 0$, 1, 10, 100, 1000 and $t - t_0 = 0.08$, 1.0, 9.0 are plotted.

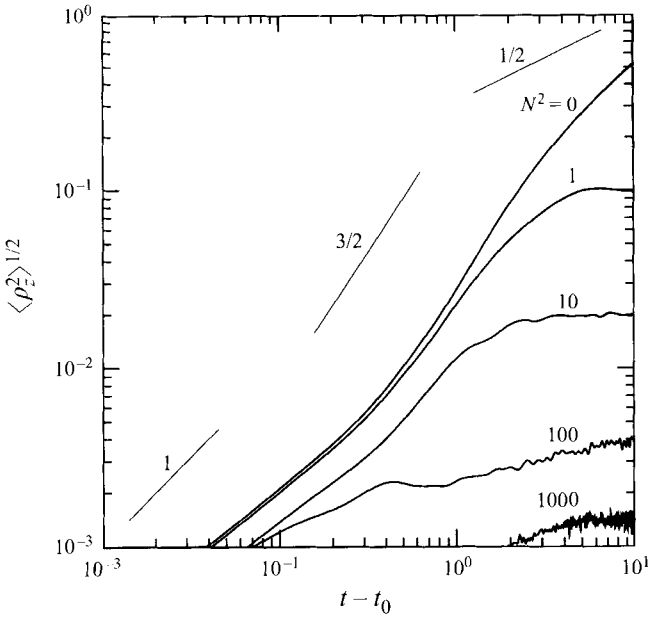

FIGURE 6. The root-mean-square of vertical dispersion of particle pairs, $\langle \rho_z^2 \rangle^{1/2}(t)$ for $N^2 = 0$, 1, 10, 100, 1000.

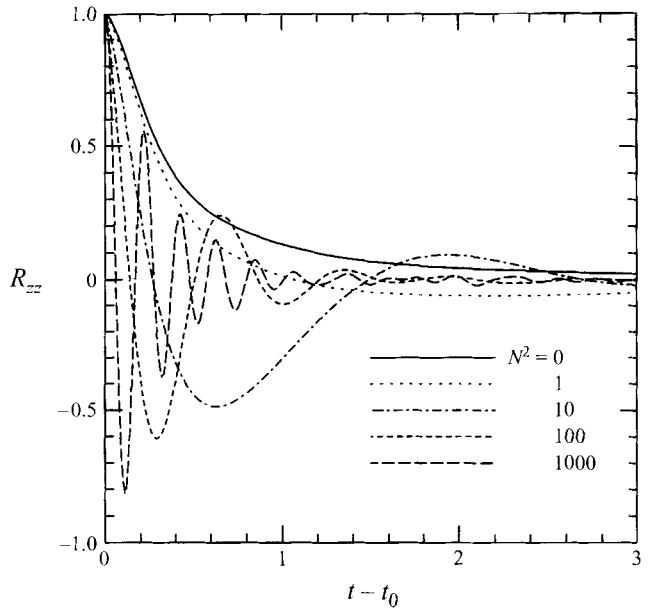

FIGURE 7. Lagrangian covariance for $N^2 = 0$, 1, 10, 100, 1000.

Figure 7 shows $R_{zz}(\tau, t_0)$ for several values of N^2, and for $t_0 = 1$. The time dependence is not dissimilar to

$$R_{zz}(\tau, t_0) \sim e^{-\mu\tau}\cos(\alpha\tau + \beta) \tag{3.11}$$

as suggested by Csanady (1964) for stationary turbulence. However, what is really needed to get particle displacements is $R_{zz}(\tau, t_0)$, where $(-t_0 \leqslant \tau \leqslant 0)$, i.e. an

integration into the past from the time of observation, t_0 in (3.11). However, we have at present no stable integration techniques for this quantity.

4. DNS eddy diffusion and its modelling

We now examine the possible relationship of the numerical results of §3 for $\langle Z^2\rangle(t)$ to Langevin estimates drawn from the statistical theory of turbulence. The Langevin model that we consider estimates the Lagrangian velocity by

$$\frac{\mathrm{d}w}{\mathrm{d}t} = -\mu_1(t)w + f(t) + \theta, \tag{4.1}$$

$$\frac{\mathrm{d}\theta}{\mathrm{d}t} = -\mu_2(t)\theta - N^2 w, \tag{4.2}$$

where $f(t)$ is a white-noise forcing function, and $\mu_1(t), \mu_2(t)$ are decorrelation rates. (In the following analysis, we set $\mu_1 = \mu_2 = \mu(t)$, for simplicity. We have repeated the calculations and analysis for the case $\mu_1 \neq \mu_2$, and we discuss briefly the differences such a change makes at the end of this section.) Here, $f(t)$ represents the pressure-gradient force. Its representation as a random force has been justified by the fact that it originates from fluctuations that are some distance from the particle, and are hence uncorrelated with it (It is interesting to note that both single-point distribution functions for the pressure and its gradient appear to be insensitive to the strength of the stratification, according to our DNS.). We must add to (4.1)–(4.2) information assured by the overall conservation laws of total energy associated with (2.1)–(2.3). For the present model, we find, from (4.1) and (4.2), the quadratic constraints

$$\frac{1}{2}\left\langle \frac{\mathrm{d}}{\mathrm{d}t}\{w^2 + N^{-2}\theta^2\}\right\rangle = -\mu(t)\langle w^2 + N^{-2}\theta^2\rangle + \sigma(t) \tag{4.3}$$

with $\langle f(t')f(t)\rangle = \sigma(t)\delta(t-t')$. (A more consistent modelling would perhaps start from a Langevin spectral model for $\partial w(\boldsymbol{k}, t) = \cdots$, as represented by an EDQNM such as the test field model (Kraichnan 1971).) Notice that in (4.1), we have explicitly included a damping term in modelling the Lagrangian velocity. On this point, we differ from the early work of Csanady (1964), in which such a term is omitted. Its omission implies that for the unstratified case ($N = 0$), and for stationary forcing, $\langle w^2\rangle$ increases linearly with time. Equation (4.1), with the μw term, is thus more analogous to what would be derived from the test field model, which proposes spectral equations (for $\boldsymbol{u}$, and θ) that contain both random forcing and damping terms for both the velocity and scalar fields. The role of the damping terms is to provide energy and entropy conservation by nonlinear terms. We can obtain the analytic solution of (4.1) and (4.2) with the initial condition $w(0) = w_0$, and $\theta(0) = 0$ as

$$w(t) = w_0 \cos Nt \exp - \int_0^t \mathrm{d}t'\mu(t') + \int_0^t \mathrm{d}s f(s) \cos N(t-s) \exp - \int_s^t \mathrm{d}t'\mu(t'), \tag{4.4}$$

$$\theta(t) = -\int_0^t N\mathrm{d}s f(s) \sin N(t-s) \exp - \int_s^t \mathrm{d}t'\mu(t'), \tag{4.5}$$

and from the above solution,

$$\langle Z^2\rangle(t) = \int_0^t \mathrm{d}s\sigma(s)\left\{\int_s^t \mathrm{d}t' g(t', s)\right\}^2 + \langle w_0^2\rangle\left\{\int_0^t \mathrm{d}t' g(t', 0)\right\}^2 \tag{4.6}$$

where $g(t, s)$ is the Green's function,

$$g(t,s) = \cos[N(t-s)] \exp - \int_s^t \mathrm{d}t' \mu(t'). \tag{4.7}$$

We may test the validity of models such as (4.1)–(4.2) by using in (4.6) the DNS constraint imposed by (4.3). In implementing this step, we should use smoothed values of $\langle w^2 \rangle$ and $\langle \theta^2 \rangle$, thereby eliminating any spurious rapid fluctuations of σ. The value of $\mu(t)$ and its dependence on N is as yet open. Physically, $\mu(t)$ represents the Lagrangian decorrelation time of the flow, and for unstratified flow we would expect it to be $\sim -\dot{E}/E$. But its dependence on N is not at all clear. We may note, in this connection, that for stationary turbulence (σ and μ independent of time), (4.6) implies that $Z^2(t) \to (\sigma\mu^2/N^4)t$, for $\mu/N \to 0$). Such a limit seems qualitatively smaller than previous theoretical estimates (Cox, Nagata & Osborn 1969; Lilly, Walko & Adelfang 1974; Weinstock 1978), all of which argue for $\langle Z^2 \rangle(t) \sim (\mu/N^2)t$. Their result is also implied by a simple closure prescription: modify the Kraichnan (1976) formula for eddy conductivity ($\kappa_{eddy} = (\frac{2}{3}) \int_0^\infty \mathrm{d}k E(k)/\eta(k)$, replacing the lower limit by $k_O \equiv ((N^3/\epsilon)^{1/2})$, so that only scales smaller than the Ozmidov scale participate in dispersion of particles. Thus, the Langevin model (4.1)–(4.2) may be reconciled with earlier theoretical estimates if

$$\mu(t) \sim N, \quad N \to \infty. \tag{4.8}$$

The above discussion suggests that

$$\mu(t) = A\dot{E}/E + BN \tag{4.9}$$

(with (A, B) arbitrary) would incorporate, roughly, the damping rate for decaying stratified flows.

A modification to Csanady's model similar to (4.9) (with only $B \neq 0$) was proposed by Pearson, Puttock & Hunt (1983) for stationary stably stratified turbulence. These authors demonstrated that the behaviour of $\langle Z^2 \rangle(t)$ after a certain time differs depending on whether there is a mechanism for interchange of density for fluid elements. In particular, if interchange of density exists, $\langle Z^2 \rangle(t)$ begins a linear growth after showing a plateau. Such a prediction agrees with the present Langevin analysis for decaying turbulence if we use $B \neq 0$.

Figure 8 shows the results of (4.6), in which $\langle w^2 \rangle(t)$ and $\langle \theta^2 \rangle(t)$ in (4.3) for $\sigma(t)$ are estimated as power-law least-square fits to the DNS decay profiles. These results are for $A = 8.0$, and $B = 0.$ in (4.9). We note a quantitative agreement between the model and the DNS results as presented in figure 4 for the larger values of N. Calculations with $B \neq 0$ typically predict that $\langle Z^2(t) \rangle$ increases as a power law in t at late time, in contradiction to the DNS of figure 4.

The reason that $B \neq 0$ in (4.9) gives poorer results is still open. As noted above, there are two avenues to a $\mu \sim N$ model: (i) an assumed damping of energy by radiation of gravity waves in the far-field, as proposed by Pearson *et al.* (1983), and (ii) as a modification of the Kraichnan eddy-diffusivity formula, suppressing diffusion by scales larger than the Ozmidov scale. Both of these assume stationary turbulence. Moreover, with regard to the first avenue, arguments for wave damping are perhaps vitiated in a periodic domain, since waves exiting the computational domain re-enter at an appropriate boundary point. Perhaps, for decaying flows, we should expect other types of parameterization for eddy-viscosity and/or eddy-diffusivity.

We have experimented with (4.1)–(4.2) for the case $\mu_1 \neq \mu_2$ (and in particular $\mu_2 < \mu_1$), with little success in improving the comparison of the model with DNS at small

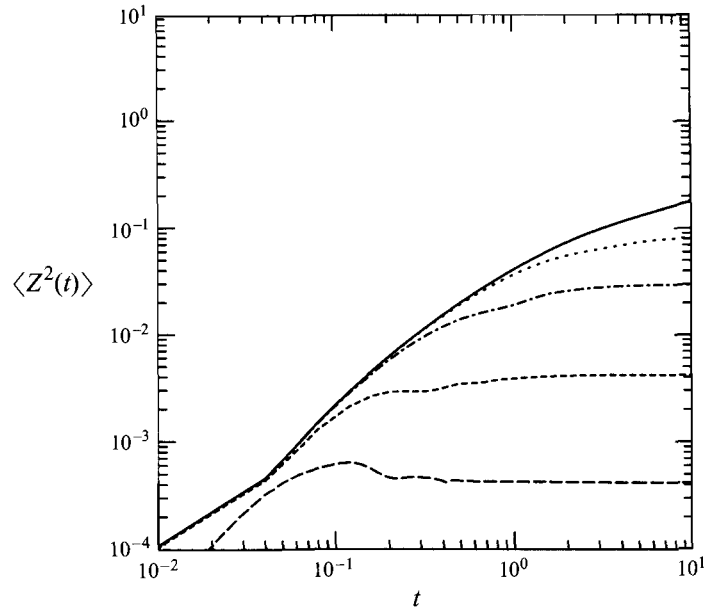

FIGURE 8. The mean-square of the vertical displacement $\langle Z^2\rangle(t)$ for $N^2 = 0$, 1, 10, 100, 1000, for the Langevin model described by (4.1)–(4.9). —, $N^2 = 0$; - - -, $N^2 = 1$; – · – · –, $N^2 = 10$; – – –, $N^2 = 100$; — — —, $N^2 = 1000$. For the curves shown, $A = 8.0$, and $B = 0$, in (4.9).

N. The only qualitative improvement is the reproduction of the $\mathrm{d}\langle Z^2\rangle/\mathrm{d}t < 0$, feature of figure 4 for large N. It is clear that if (4.1)–(4.2) is credible, a dependence of μ on N must be admitted. The data suggest a dependence such as $\mu \sim (a+bNt/(1+Nt))/t$, with $a \sim 1$, and $b \sim 7$. The combination Nt is dictated by dimensional considerations.

5. Discussion of dynamical issues

The properties of diffusion may well have a close relation with the structure of the flow field, as has been suggested by Fung *et al.* (1991). Figure 9 shows the isosurfaces of enstrophy at $t = 4$ for $N^2 = 0$, 1, 10, and 100 (the surface level is 5 times the r.m.s. value). We observe scattered pancake-shaped vortex patches lying almost in the horizontal plane. These two-dimensional pancakes contrast significantly with the vortex tubes often observed in homogeneous isotropic simulations (Siggia & Patterson 1978; Kerr 1985; She, Jackson & Orszag 1990). They also provide us with a new image of structures in stratified turbulence. Previously, simulations (Métais & Herring 1989) and experiments (Fernando 1988) showed vortex sheets that extended in the horizontal plane as a typical manifestation of two-dimensionalization of stratified turbulence. Scattered pancakes seem a good candidate for the final structures in decaying stratified turbulence.

The vertical length scale (the thickness of the patches or their vertical spacing) should be related to the Ozmidov scale (Fernando 1988). It is interesting to note that these strong enstrophy regions are strong vertical-shear regions, and this is verified by checking the direction of vorticity vectors in these regions. Figure 10 illustrates the distribution of the polar angle of vorticity vectors,

$$\Theta = \cos^{-1}\left\{\frac{\omega_z}{(\omega_x^2+\omega_y^2+\omega_z^2)^{1/2}}\right\}, \tag{5.1}$$

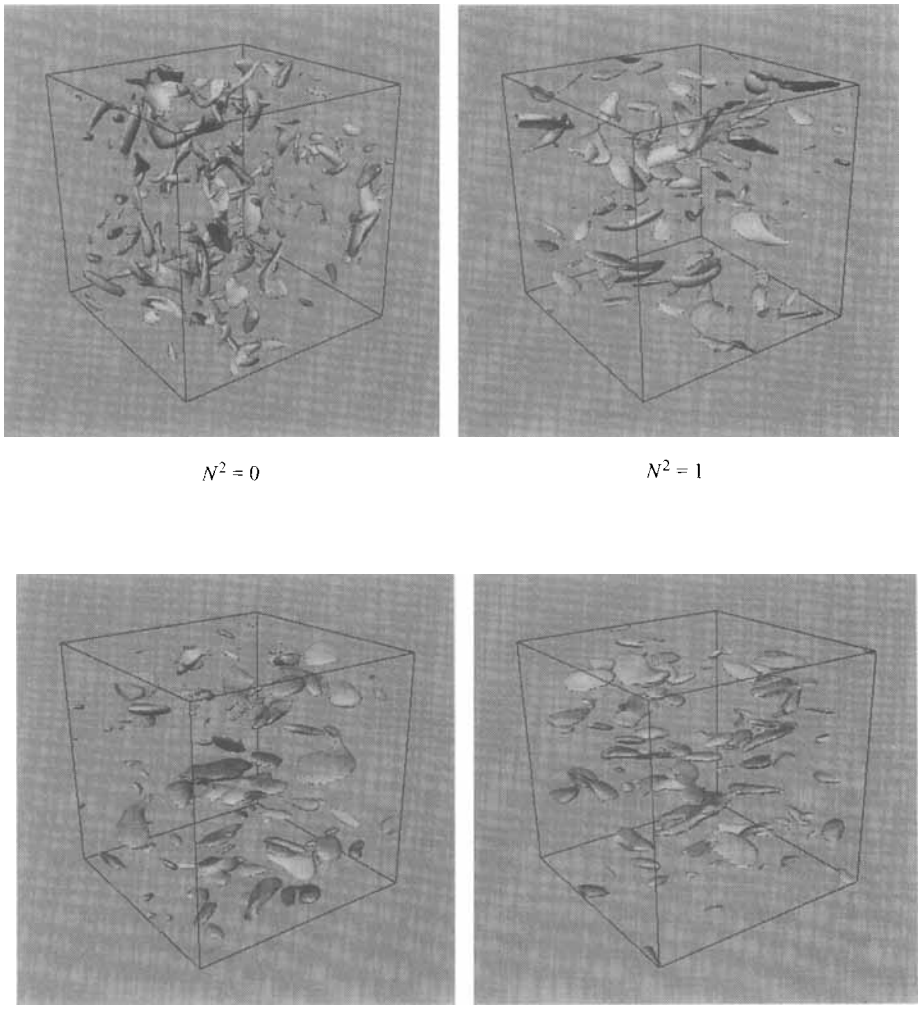

FIGURE 9. Isosurfaces of enstrophy for $N^2 = 0$, 1, 10, 100 at $t = 4.0$. The contour level is four times the root-mean-square enstrophy.

for several values of N^2 (normalized by $2\pi\sin\Theta$). Vorticity vectors are more horizontal for higher stratification. Furthermore, we observe that vectors with larger magnitude tend to be more horizontal.

Figure 11 illustrates the isosurface of the z-component of vorticity and vortex lines starting from a positive vortex blob. Three groups of vortex lines are shown. Those in group (*a*) are chaotic. Since the figure is made from a snap shot of the vorticity field, this is a space projection of the space-temporal chaos. In spite of the concordance in shapes and positions of vortex lines, the initial small difference in the position is amplified gradually, and the lines separate significantly later.

Group (*b*) contains vortex lines which connect to another strong vertical-vorticity region. In addition the vortex lines get bent just outside the blobs due to the strong shear. This group verifies one of the categories of vortex network (positive–positive) suggested by Fincham, Maxworthy & Spedding (1994). The group (*c*) seems exotic.

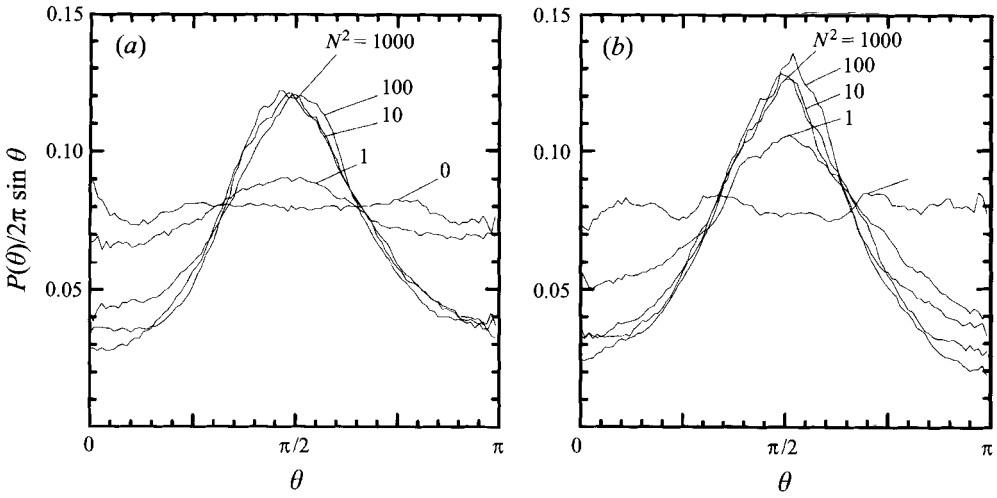

FIGURE 10. Polar angle distribution of vorticity vectors. (*a*) $t = 5$, (*b*) $t = 10$.

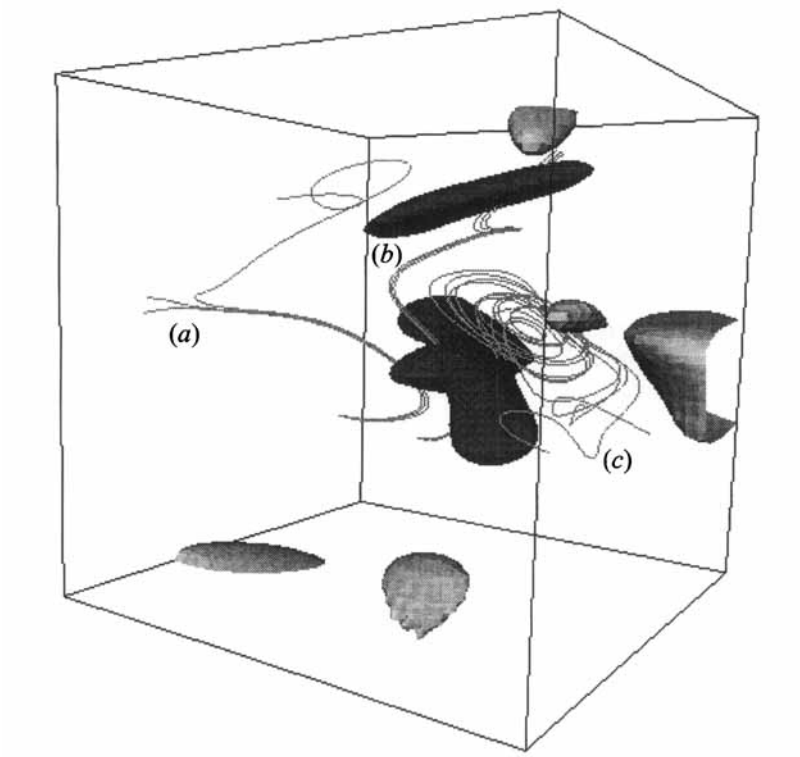

FIGURE 11. Typical groups of vortex lines starting from a strong positive vertical vorticity region (centred, dark) for $N^2 = 100$ at $t = 10.0$: (*a*) (spatially) chaotic vortex lines that are sensitive to small initial differences in space, (*b*) vortex lines which connect to another strong positive region (dark above) after being bent by the strong shear in between, (*c*) vortex lines which connect to a strong negative region (light next to the centred) and come back to the positive one, which iterates.

The vortex lines starting from the positive region are diverted by the shear toward a strong negative region and then pulled into it. These vortex lines are an example of another category of the vortex network (positive–negative). It is most surprising that these vortex lines return toward the positive blob again, making a loop between the positive and negative blobs. This loop is repeated several times as if they formed a coil of vortex lines or an assembly of vortex rings. The case (*c*), being maybe a rare event, implies the possibility of the induction of a strong jet penetrating the coil.

The paper by Fincham *et al.* (1994) addressed the question of why, under stable stratification, large-scale (vertical) vortices cannot be produced, and conjectured that the strong shear bends vortex lines horizontally and keeps them from connecting strong vertical-vorticity regions. Along with this conjecture, they proposed several possible connections of vortex lines called the vortex network. All such categories of connections have been verified in our present simulations. Furthermore, we observed that the direction of horizontal shear flow is random, which results in the three-dimensional (spatial) chaos of vortex lines and randomly scattered pancake-shaped vortices.

If rotation is imposed in addition to stratification, it has been reported that the inverse cascade of energy is enhanced to generate large vertically coherent vortices (Métais *et al.* 1996; McWilliams, Weiss & Yanneh 1994) For the generation of coherent vortices, rotation should be strong enough to compensate for the decorrelation of velocity in the vertical direction which is the main characteristic of stable stratification. The properties of particle diffusion under stratification and rotation are another topic in the study of geostrophic turbulence, and will be reported elsewhere. In particular, the effect of coherent structure on diffusion requires new insights both theoretically and experimentally.

6. Conclusions

In this paper, we have examined stably stratified turbulence, and the effect of stratification on dispersion of particles borne by the flow. We have explored the regime of very strong stratification, for which some form of asymptotics may possibly be valid. Our tool has been DNS for decaying turbulence, perforce at modest Reynolds numbers. We have chosen to examine decaying rather than stationary flow because of its cleanness: stationary flow would require a mean shear or stirring mechanism for its maintenance, either of which would introduce complications in the flow. However, traditional methods of analysing dispersion by turbulence are formulated for stationary flow. Therefore to make comparisons of DNS results with statistical models (such as that of Csanady 1964), we have extended the latter for decaying flows, and taken its parameters (such as energy and dissipation) from the DNS. Such phenomenological theories model the particle acceleration as a damped oscillator, with a random force, which represents pressure fluctuations along the particle trajectories. Both more refined versions of the Csanady model (such as that of Fung *et al.* 1991) and qualitative reasoning drawn from statistical theories (such as Weinstock 1978) suggest a damping depending linearly on the Brunt–Väisälä frequency, whereas our DNS results (at very large N) suggested a damping rate independent of N. Thus, we find a much weaker dispersion of particles than classical theories would indicate. The weak, or even negative, dispersion of particle pairs found here is surprising, but perhaps not unanticipated. For example, Taylor (1921) in his classic paper notes that such constriction of particle trajectories may occur, and

associates the constriction with a Lagrangian correlation function of the sort given by figure 5. We should also note the study of Riley & Metcalfe (1990), who found a striking inhibition of diffusion of a turbulent fluid initially confined in a narrow horizontal band within a stable region.

There remains the question of why our results indicate a much weaker eddy diffusion than classical estimates. Perhaps a clue to this dilemma is to be found in our discussion following (4.7) of how the classical formula may be obtained from a simple closure prescription for eddy conductivity. There, we noted that the classical $\kappa_{eddy} = \mu/N^2$ is obtained by suppressing those scales larger than the Ozmidov scale ($k_O = (N^3/\epsilon)^{1/2}$), whose dominantly oscillatory motions contribute little to diffusion. A glance at figure 1(*b*) suggests that for most of the cases we have investigated, k_O is quite large, and hence there is little energy at scales $< 1/k_O$, the domain of near-isotropic turbulence that would contribute to vertical mixing.

The enstrophy distribution of the turbulence for strong stratification resembles scattered pancakes. We do not see the vortex filaments that are the distinguishing features of the small scales of isotropic turbulence. The pancakes are consistent with an angular distribution of vorticity vectors strongly peaked in the horizontal plane. The numerical results suggest that the shape of this angular distribution may become asymptotic with $N \to \infty$. Such a distribution is inconsistent with the notion that strongly stratified turbulence is similar to two-dimensional turbulence, since energy dissipation at small scales is dominated by horizontal vorticity, a component missing from two-dimensional dynamics. Our results here are similar to the experiments of Fincham *et al.* (1994) and are in agreement with earlier studies by Métais & Herring (1989) and Herring & Métais (1989).

We are grateful to Dr Jeffrey Weil for many useful discussions. We are also grateful to Drs Shuman Du, P. K. Yeung, and Peter Sullivan for critically reading an earlier version of the manuscript, and for constructive suggestions. Part of this work was completed while the second author was a visiting Professor at the Laboratoire de Modelisation en Mécanique à l'Université Pierre et Marie Curie. NCAR is sponsored by the National Science Foundation.

REFERENCES

Britter, R. E., Hunt, J. C. R., Marsh G. L. & Snyder, W. H. 1993 The effects of stable stratification on the turbulent diffusion and the decay of grid turbulence *J. Fluid Mech.* **127**, 27–44.

Cox, C. Y., Nagata, Y. & Osborn, T. 1969 Oceanic fine structure and internal waves. Papers in dedication to Prof. Michitaka Uda. *Bull. Japan Soc. Fish. Oceanogr. Tokyo* **1**, 67–71.

Csanady, G. T. 1964 Turbulent diffusion in a stratified fluid. *J. Atmos. Sci.* **21**, 439–447.

Fernando, H. J. S. 1988 On the oscillations of harbors of arbitrary shape. The growth of a turbulent patch in a stratified flow. *J. Fluid Mech.* **190**, 55–70.

Fincham, A., Maxworthy, M. T. & Spedding, G. R. 1994 The horizontal and vertical structure of the vorticity field in freely-decaying, stratified grid-turbulence. In *Preprints, 4th Symp. on Stratified Flows*, vol. 2, § A4.

Fung, J. C. F., Hunt, J. C. R., Malik, N.A. & Perkins, R. J. 1991 Kinematic simulation of homogeneous turbulence by unsteady random Fourier modes. *J. Fluid Mech.* **236**, 281–318.

Godeferd, F. S. & Cambon, C. 1994 Detailed investigation of energy transfer in homogeneous stratified turbulence. *Phys. Fluids* A **6**, 2084–2100.

Herring, J. R. 1988 The inverse cascade range of quasigeostrophic turbulence *Met. Atmos. Phys.* **38**, 106–115.

HERRING, J. R. & MÉTAIS, O. 1989 Numerical experiments in forced stably stratified turbulence. *J. Fluid Mech.* **202**, 97–115.

HERRING, J. R. & MÉTAIS, O. 1992 Spectral transfer and bispectra for turbulence with passive scalars. *J. Fluid Mech.* **235**, 103–121.

HERRING, J. R., SCHERTZER, D., LESIEUR, M., NEWMAN, G. R., CHOLLET, J.-P. & LARCHEVEQUE, M. 1982 A comparative assessment of spectral closure as applied to passive scalar diffusion. *J. Fluid Mech.* **124**, 411–437.

KERR, R. M. 1985 Higher order derivative correlations and the alignment of small-scale structures in isotropic numerical turbulence. *J. Fluid Mech.* **153**, 31–58.

KIMURA, Y. 1992 Intermittency growth in 3D turbulence. In *Proc. of NATO Advanced Research Workshop on Topological Fluid Dynamics* (ed. H. K. Moffatt, R. M. Zaslavsky, M. Tabor & P. Comte). pp. 401–413. Kluwer.

KIMURA, Y. & HERRING, J. R. 1995 *Stratified Turbulence: Structural Issues, and Turbulent Diffusion* (ed. M. Meneguzzi, A. Pouquet & P. L. Sulem). Lecture Notes in Physics, vol. 462, pp. 195–204. Springer.

KOLMOGOROV, A. N. 1942 On degeneration of isotropic turbulence in an incompressible viscous liquid. *Dokl. Akad. Nauk. SSSR* **31**, 538–541.

KRAICHNAN, R. H. 1971 An almost markovian Galilean invariant turbulence model *J. Fluid Mech.* **47**, 513–524.

KRAICHNAN, R. H. 1976 Eddy viscosity in two- and three-dimensional turbulence. *J. Atmos. Sci.* **33**, 1521–1536.

LEITH, C. E. 1967 Diffusion approximation to the inertial energy transfer in isotropic turbulence. *Phys. Fluids* **10**, 1409–1416.

LESIEUR, M. 1990 *Turbulence in Fluids*, 2nd edn. Kluwer.

LESIEUR, M. & SCHERTZER, D. 1978 Amortissement auto similarité d'une turbulence à grand nombre de Reynolds. *J. Méc.* **17**, 609–646.

LILLY, D. K., WALKO, D. E. & ADELFANG, S. I. 1974 Stratospheric Mixing estimated from high-altitude turbulence measurements. *J. Appl Met.* **13**, 488–493.

MCWILLIAMS, J. C., WEISS, J. B. & YAVNEH, I. 1994 Anisotropy and coherent vortex structures in planetary turbulence *Science* **264**, 410–413.

MÉTAIS, O., BARTELLO, P., GARNIER, E., RILEY, J. J. & LESIEUR, M. 1996 Inverse cascade in stably stratified rotating turbulence. *Dyn. Atmos. Oceans* **23**, 193–203.

MÉTAIS, O. & HERRING J. R. 1989 Numerical studies of freely decaying homogeneous stratified turbulence. *J. Fluid Mech.* **202**, 117–148.

ORSZAG, S. A. & PATTERSON, G. S. 1972 Numerical simulation of turbulence. In *Statistical Models of Turbulence* (ed. M. Rosenblatt & C. Van Atta), pp 127–147. Springer.

PEARSON, H. J., PUTTOCK, J. S. & HUNT, J. C. R. 1983 A Statistical model of fluid-element motions and vertical diffusion in a homogeneous stratified turbulent flow. *J. Fluid Mech.* **129**, 219–249.

RILEY, J. J. & METCALFE, R. W. 1990 Direct numerical simulations of turbulent patches in stable-stratified fluids. In *Stratified Flows* (ed. E. J. List & G. H. Jirka), pp. 541–549. ASME.

RILEY, J. J., METCALFE, R. W. & WEISSMAN, M. A. 1982 Direct numerical simulations of homogeneous turbulence in density stratified fluids. In *Proc. AIP Conf. on Nonlinear Properties of Internal Waves*, pp. 679–712.

SHE, Z.-S., JACKSON, E. & ORSZAG, S. A. 1991 Structure and dynamics of homogeneous turbulence: models and simulation. *Proc R. Soc. Lond.* A **434**, 101–124.

SIGGIA, E. D. & PATTERSON, G. S. 1978 Intermittency effects in a numerical simulation of stationary turbulence. *J. Fluid Mech.* **86**, 567–592.

TAYLOR, G. I. 1921 Diffusion by continuous motion. *Proc. Lond. Math Soc.* **20**, 10–25.

WEINSTOCK, J. 1978 Vertical turbulent diffusion in a stably stratified fluid. *J. Atmos. Sci.* **35**, 1022–1027.

YEUNG, P. K. & POPE, S. B. 1989 Lagrangian statistics from direct numerical simulations of isotropic turbulence. *J. Fluid Mech.* **207**, 531–586.

YEUNG, P. K. & ZHOU, Y. 1995 Two dimensionalization and spectral transfer in rotating turbulence *Bull. Am. Phys. Soc.* **40**.

ZHOU, Y. 1995 A phenomenlogical treatment of rotating turbulence *Phys. Fluids* **7**, 2092–2094.